

# Perovskite Solid-State Electrolytes for Lithium Metal Batteries

Subjects: **Energy & Fuels**

Contributor: Shuo Yan

Solid-state lithium metal batteries (LMBs) have become increasingly important in recent years due to their potential to offer higher energy density and enhanced safety compared to conventional liquid electrolyte-based lithium-ion batteries (LIBs). However, they require highly functional solid-state electrolytes (SSEs) and, therefore, many inorganic materials such as oxides of perovskite  $\text{La}_{2/3-x}\text{Li}_3\text{xTiO}_3$  (LLTO) and garnets  $\text{La}_3\text{Li}_7\text{Zr}_2\text{O}_{12}$  (LLZO), sulfides  $\text{Li}_{10}\text{GeP}_2\text{S}_{12}$  (LGPS), and phosphates  $\text{Li}_{1+x}\text{Al}_x\text{Ti}_{2-x}(\text{PO}_4)_{3x}$  (LATP) are under investigation. Among these oxide materials, LLTO exhibits superior safety, wider electrochemical window (8 V vs. Li/Li<sup>+</sup>), and higher bulk conductivity values reaching in excess of  $10^{-3}$  S cm<sup>-1</sup> at ambient temperature, which is close to organic liquid-state electrolytes presently used in LIBs.

safety

perovskite

ceramic

solid-state electrolytes

LLTO

tape casting

lithium metal batteries

## 1. Introduction

It is widely believed that the most efficient strategy to achieve meaningful reduction in greenhouse gas (GHG) emissions is by electrification of transportation and expanding the use of renewable energy sources. Both of these approaches require transformative energy storage technology [1][2][3][4][5][6]. One of the most promising energy storage technologies is solid-state lithium batteries (LBs) [7][8][9][10]. LBs are rechargeable, and they were first introduced on the market by Sony Corporation in 1991 [11]. One of the key distinctions of LBs is that they have a much higher energy density than conventional nickel-cadmium (Ni-Cd) [12], lead-acid (Pb-acid) [12], nickel-hydrogen (Ni-H<sub>2</sub>) [13], and silver-zinc (Ag-Zn) [14] batteries represented in a Ragone plot (**Figure 1**).

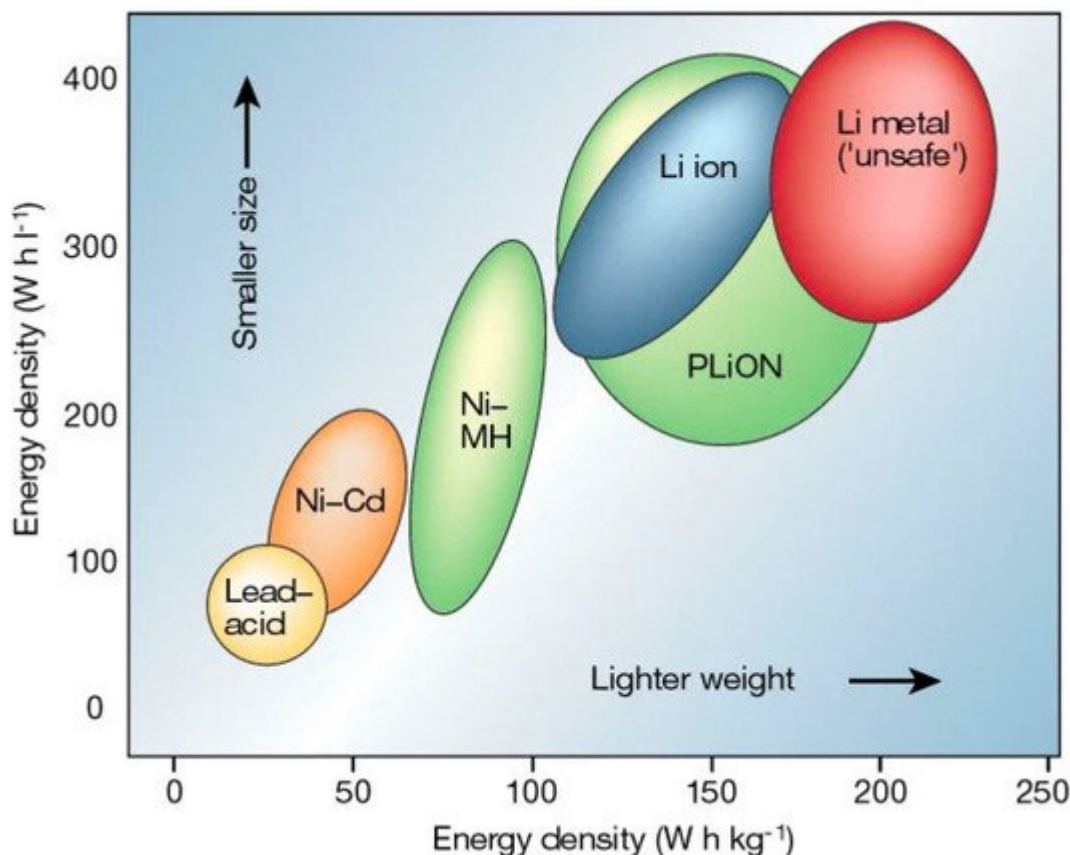


**Figure 1.** Ragone plot of lithium batteries [15].

However, another safety issue common for conventional LBs is the high flammability and low thermal stability of organic liquid-state electrolytes [16][17][18][19]. This issue can be solved by substituting solid-state electrolytes (SSEs) in place of liquid-state electrolytes [20][21][22]. Solid oxide electrodes and electrolytes enable energy/power cells to operate at a higher temperature range and accelerate reactions at the cathode and anode, leading to a higher discharging/charging rate. In addition, SSEs have wider electrochemical windows that increase their adaptiveness to high-voltage cathode materials and lithium-metal anodes, which can also enhance the energy density (up to 70% [23]) and cycling performance of LBs. When combined with a lithium metal anode and Ni-rich oxide ceramic cathode, SSEs can enable the safest batteries with the highest energy density to meet the demand for electrification of air and surface transportation [24].

SSEs include polymer, inorganic (e.g., ceramic-based oxide electrolytes) and hybrid electrolytes. Free-standing polymer electrolytes could be prepared with proper crosslinkers [25][26][27][28][29] followed by photopolymerization as an in-situ approach [30][31][32][33][34]. Fabricated gel polymer electrolytes are capable of creating high-quality interfacial contact with electrodes and good electrochemical properties [35]. Besides, Li et al. [36] and Yao et al. [37] presented recently progress on polymer-based electrolytes. Unfortunately, they still have limited ionic conductivity at room temperature. Inorganic oxides SSEs mainly include perovskites, garnets, NASICON-type, and LISCON-type [38]. Cao et al. [38] comprehensively reviewed inorganic SSEs for lithium batteries. Similar to perovskites, hybrid polymer-ceramic systems utilize ceramic fillers with garnets as a dispersant into the polymer matrix (i.e.,

poly (ethylene oxide) (PEO)-based, polyacrylonitrile(PAN)-based, polyvinylidene fluoride (PVDF)-based, etc.) [39]. Goodenough et al. [40] fabricated low-cost hybrid PEO-LLZTO electrolytes and applied them in LiFePO<sub>4</sub>|Li cells that delivered high discharge capacity (139.1 mAh g<sup>-1</sup> with capacity retention of 93.6% after 100 cycles). Falco et al., innovatively prepared cross-linked hybrid electrolytes to enhance ionic conductivity by mixing LLZO, lithium bis(trifluoromethanesulfonyl) imide (LiTFSI), tetra (ethylene glycol dimethyl ether) (G4) together under UV-light [41] [42]. The hybrid electrolytes exhibited excellent ionic conductivity of 0.1 mS cm<sup>-1</sup> at 20 °C. Passerini's group [43] presented UV cross-linked PEO polymer electrolytes [44] with ionic liquids. The room temperature ionic conductivity could reach nearly 10<sup>-3</sup> S cm<sup>-1</sup>.

We summarized the progress of LLTO electrolytes in solid-state LBs (as shown in **Figure 2**). Many investigations have been undertaken on LLTO composite SSEs and electrochemical performance of selected electrolytes are summarized in the **Table 1**. However, hybrid electrolytes still suffer safety issues due to the flammability of the organic polymers. There is few research working on 100% ceramic electrolytes in solid-state LBs applications.

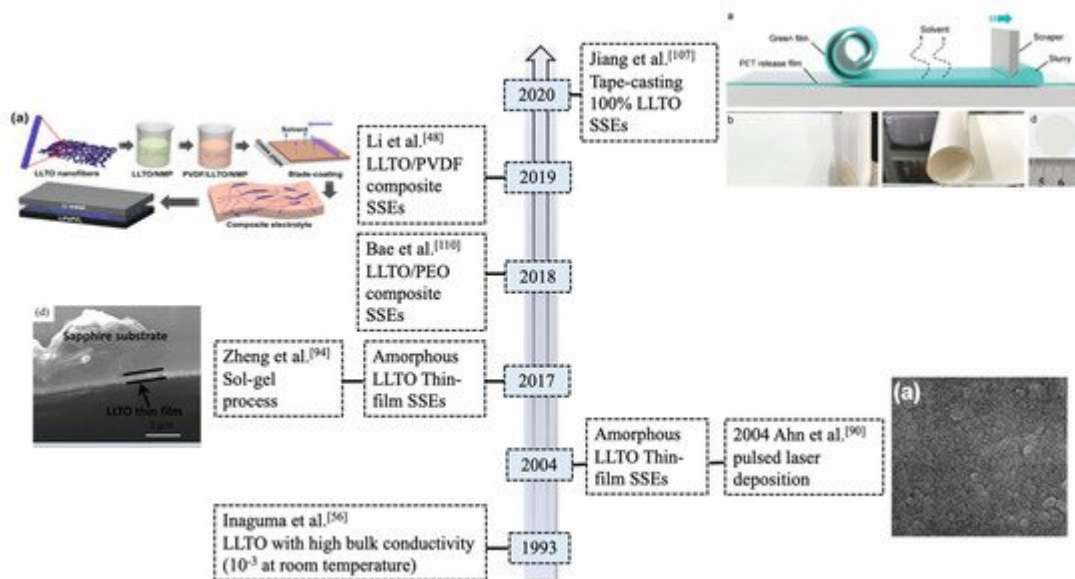


**Figure 2.** Timeline for the development of typical LLTO ( $\text{La}_{2/3-x}\text{Li}_{3x}\text{TiO}_3$ ) solid-state electrolytes (SSEs) in lithium metal batteries.

**Table 1.** Summary of electrochemical performance for selected LLTO SSEs in LBs.

SSEs Composition	Anode Cathode	Ionic Conductivity (S cm <sup>-1</sup> )	Discharge Capacity/Charging rate/Cycle Number (Capacity Retention Rate)
LLTO/ <sup>1</sup> PAN/ <sup>2</sup> SN [45]	Li LiFePO <sub>4</sub>	$2.20 \times 10^{-3}$ at 30 °C	151 mAh g <sup>-1</sup> C/2 150 (data unavailable)

SSEs Composition	Anode Cathode	Ionic Conductivity ( $\text{S cm}^{-1}$ )	Discharge Capacity/Charging rate/Cycle Number (Capacity Retention Rate)
LLTO/ <sup>3</sup> PEO/LiTFSI/SN [46]	Li NMC 532	$>10^{-3}$ at 55 °C	143.2 mAh g <sup>-1</sup> C/20 30 (data unavailable)
LLTO/PEO [47]	Li LiFePO <sub>4</sub>	$3.31 \times 10^{-4}$ at <sup>7</sup> RT	147 mAh g <sup>-1</sup> C/10 100 (~98%)
15 wt.% LLTO/ <sup>4</sup> PVDF [48]	Li LiFePO <sub>4</sub>	$5.3 \times 10^{-4}$ at 25 °C	121 mAh g <sup>-1</sup> 1C 100 (~99%)
LLTO/PEO/LiTFSI [49]	Li LiFePO <sub>4</sub>	$1.3 \times 10^{-4}$ at 60 °C	144.6 mAh g <sup>-1</sup> 1C 100 (~96%)
LLTO/PEO/LiTFSI [50]	Li LiFePO <sub>4</sub>	$1.6 \times 10^{-4}$ at 60 °C	135 mAh g <sup>-1</sup> 2C 300 (79%)
5 wt.% LLTO/PEO/LiTFSI [51]	Li LiFePO <sub>4</sub>	$3.63 \times 10^{-4}$ at 60 °C	123 mAh g <sup>-1</sup> C/2 100 (94%)
8 wt.% LLTO/PEO/ <sup>5</sup> PPC/LiTFSI [52]	Li LiFePO <sub>4</sub>	$4.72 \times 10^{-4}$ at 60 °C	135 mAh g <sup>-1</sup> C/2 100 (96%)
3wt.% LLTO/PEO/LiClO <sub>4</sub> [53]	Li LiFePO <sub>4</sub>	$4.01 \times 10^{-4}$ at 60 °C	140 mAh g <sup>-1</sup> 1C 100 (92.4%)
LLTO/ <sup>6</sup> BC [54]	Li LiFePO <sub>4</sub>	$1.54 \times 10^{-3}$ at RT	151.7 mAh g <sup>-1</sup> C/5 100 (98.5%)
Sr/Ta co-doped LLTO [55]	Li LiFePO <sub>4</sub>	$1.40 \times 10^{-4}$ at 25 °C	83.8 mAh g <sup>-1</sup> C/10 $-3.80 (89\%)^{-1}$ nperature

as shown in **Figure 3a** and low electronic conductivity [56] (i.e.,  $10^{-8}$  S cm<sup>-1</sup>). Inaguam et al. [57] was the first to report LLTO solid-state electrolytes (SSEs) with relatively high bulk ionic conductivity (i.e.,  $1 \times 10^{-3}$  S cm<sup>-1</sup> at room temperature) and total ionic conductivity (i.e.,  $>2 \times 10^{-5}$  S cm<sup>-1</sup> at room temperature). **Figure 3b** shows the

Arrhenius plots of the ionic conductivities of the perovskite compared with other ceramic SSEs. Thus, LLTO has been widely used as an additive within polymers to form composites for ionic conductivities enhancement.

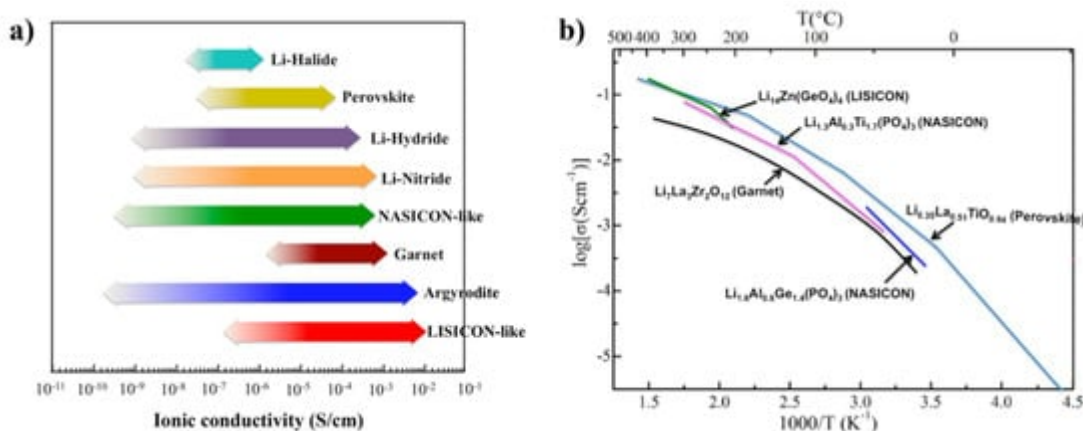


**Figure 3.** (a) Typical SSEs with highly ionic conductivities at room temperature; and (b) ionic conductivities of selected SSEs with elevated temperature. Reprinted (adapted) with permission from [56]. Copyright 2017 American Chemical Society.

In general, LLTO has many advantages: (1) large ionic transference numbers (i.e., 0.5~0.9); (2) superior chemical and thermal stability in air; and (3) environmental friendliness without any release of toxic gases during decomposition reactions. Besides, LLTO SSEs show wide electrochemical windows (8 V vs. Li/Li<sup>+</sup>) that increase their adaptiveness to high-voltage cathode materials and if combined with lithium-metal anodes. Also, LLTO exhibits excellent thermal stability (4–1600 K [58]) that provide potential applications even at extreme conditions.

However, there are several challenges that hamper the application of LLTO SSEs in batteries. First of all, the large grain boundary resistance reduces total ionic conductivity below  $10^{-5}$  S cm<sup>-1</sup> at room temperature [58]. Secondly, LLTO is chemically unstable when in direct contact with lithium metal. Lithium can be intercalated into LLTO at voltages below about 1.8 V, which causes the Ti<sup>4+</sup> reduction and enhanced electronic conductivity [58]. Thirdly, the brittleness nature of LLTO makes it hard to fabricate and assemble into batteries. Besides, due to internal volume changes of batteries during operation, delamination of the ceramic oxide electrode and electrolyte layers can occur, causing the battery life to be shortened [59].

In this review, we presented and analyzed the origins of large grain boundary resistance for LLTO and solutions. We also gained an insight to the chemical instability of LLTO electrolytes when contacts lithium-metal anode. Moreover, we reviewed the tape-casting fabrication methods and electrochemical performances for 100% amorphous and crystalline LLTO SSEs in LBs.

## 2. Crystal Structure/Composition of LLTO and Relationship to Ionic Conductivity

Perovskite  $\text{La}_{2/3-x}\text{Li}_x\text{TiO}_3$  (LLTO)-family ( $0.04 < x < 0.16$ ) with  $\text{ABO}_3$  structure (**Figure 4a,b**) has Li, La (La-rich and La-poor regions), and vacancies occupying the A sites, and Ti-ions occupying B sites that are octahedrally coordinated by oxygen [60].

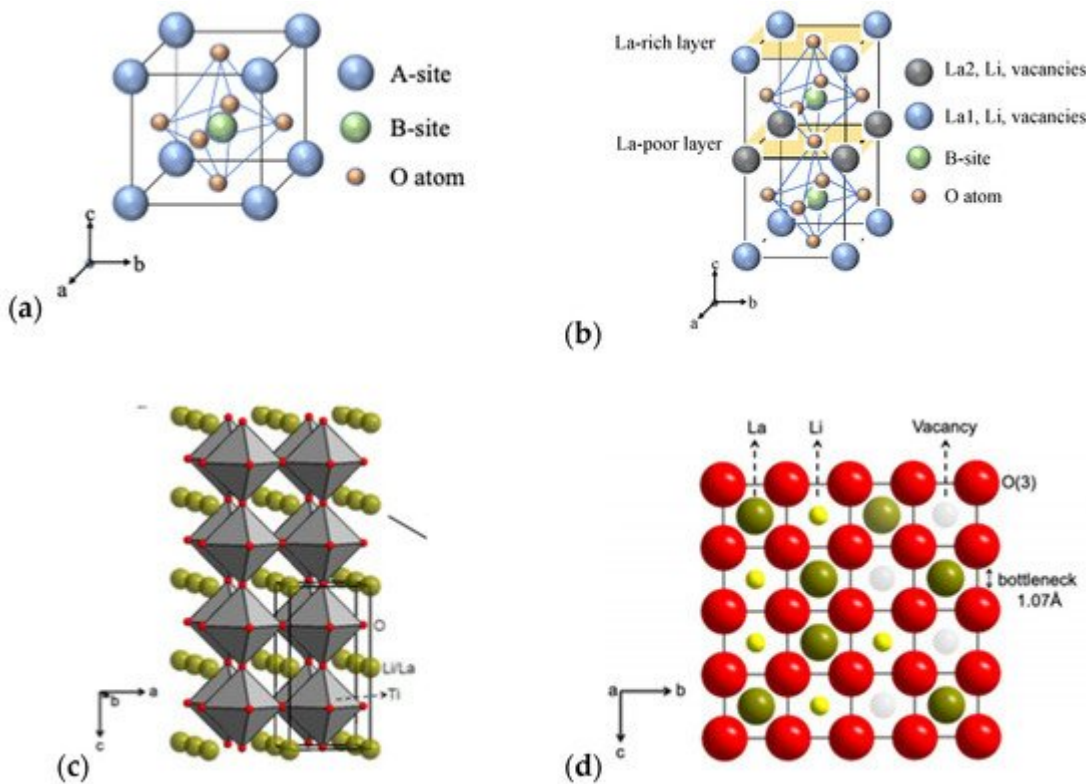


**Figure 4.** (a)  $\text{ABO}_3$  structure; (b) La-rich and La-poor regions; (c) Crystal structure of ( $P4/mmm$ )-type LLTO [60]; and (d) bottleneck structure of 12-fold coordinated with oxygen ions [60].

**Figure 4c** indicates the crystal structure of the tetragonal-type perovskite with the lattice parameter of  $a = 3.8 \text{ \AA}$  [60] for cubic unit cell. Various  $x$  values of the lithium and lanthanum lead to distorted structures which generally originates from the unequal distribution of vacancies and displaced cations of  $\text{Li}^+$  and  $\text{La}^{3+}$ . The bottleneck structure of perovskites consists of 12-fold coordinated with corner-shared oxygen as shown in **Figure 4d** [60]. The stable structure could be maintained when the  $x$  value is between 0.04 and 0.16.

Cubic and tetragonal LLTO ( $x \approx 0.11$ ) display a lattice structure with the stacking of La-rich and La-poor regions (**Figure 4b**) to maintain high bulk conductivity [60]. Inaguma and Itoh [61] showed that the conductivity of LLTO solid solution shows a parabolic dependence on  $x$  due to variations in the lithium to vacancy concentration and the formation of low activation energy pathways for ions controlled by site percolation and bottleneck size.

A lot of research has been dedicated to perovskite-type electrolytes to better understand the relationship of the chemical composition, crystal structure, and synthetic methods on lithium ionic conductivity [60][61]. Many works synthesized LLTO that the content of lithium around 0.11. Proper adjustments of this value depend on dopants in LLTO. **Table 2** shows the summary of room-temperature ionic conductivities for selected LLTO SSEs (with common dopants) ionic conductivity at room temperature. The optimal  $x$  with the highest conductivity (more than  $10^{-4} \text{ S}$

$\text{cm}^{-1}$  at room temperature) was found by many researchers to be around  $\sim 0.1$  (LLTO commercial powder from TOHO TITANIUM Co., Ltd.).

**Table 2.** Summary of selected LLTO SSEs in ionic conductivities.

Composition	Space Group	Conductivity at RT ( $\text{S cm}^{-1}$ )	Synthesis Method
Type I: pure LLTO SSEs			
$\text{La}_{0.61}\text{Li}_{0.17}\text{TiO}_3$	$Cmmm$	$3.76 \times 10^{-4}$	Pulsed Laser Deposition [62]
$\text{La}_{0.5}\text{Li}_{0.5}\text{TiO}_3$	$P4/mmm$	$3.52 \times 10^{-7}$	Spin Coating [63]
	$P4/mmm$	$7.2 \times 10^{-7}$	Microwave Sintering Method [64]
Type II: composite LLTO SSEs			
$\text{La}_{0.5}\text{Li}_{0.5}\text{TiO}_3/\text{nano-Ag}$	$Pm3m$	$2.8 \times 10^{-5}$	Sol-gel Processing [65]
$\text{La}_{0.5}\text{Li}_{0.5}\text{TiO}_3/\text{silica}$	$P4/mmm$	$1 \times 10^{-4}$	Wet Chemical Method [66]
Sr-doped $\text{La}_{0.56}\text{Li}_{0.33}\text{TiO}_3$	$Pm3m$	$9.51 \times 10^{-4}$	Sol-gel Processing [67]
Y-doped $\text{La}_{0.46}\text{Li}_{0.33}\text{TiO}_3$	$P4/mmm$	$1.95 \times 10^{-3}$	Sol-gel Processing [68]
Nb-doped $\text{La}_{0.5}\text{Li}_{0.5}\text{TiO}_3$	$P4/mmm$	$1.04 \times 10^{-4}$	Solid-state Reaction Method [69]
Sr/Co-doped $\text{La}_{0.557}\text{Li}_{0.33}\text{TiO}_3$	$Pmm$	$1.4 \times 10^{-4}$	Solid-state Reaction Method [55]

## References

- Denholm, P.; Kulcinski, G.L. Life cycle energy requirements and greenhouse gas emissions from large scale energy storage systems. *Energy Convers. Manag.* 2004, 45, 2153–2172.
- Goodenough, J.B.; Kim, Y. Challenges for Rechargeable Li Batteries. *Chem. Mater.* 2010, 22, 587–603.
- Goodenough, J.B.; Park, K.-S. The Li-Ion Rechargeable Battery: A Perspective. *J. Am. Chem. Soc.* 2013, 135, 1167–1176.
- Larcher, D.; Tarascon, J.-M. Towards greener and more sustainable batteries for electrical energy storage. *Nat. Chem.* 2015, 7, 19–29.

5. Liang, Y.; Su, J.; Xi, B.; Yu, Y.; Ji, D.; Sun, Y.; Cui, C.; Zhu, J. Life cycle assessment of lithium-ion batteries for greenhouse gas emissions. *Resour. Conserv. Recycl.* 2017, 117, 285–293.
6. Liu, J.; Bao, Z.; Cui, Y.; Dufek, E.J.; Goodenough, J.B.; Khalifah, P.; Li, Q.; Liaw, B.Y.; Liu, P.; Manthiram, A.; et al. Pathways for practical high-energy long-cycling lithium metal batteries. *Nat. Energy* 2019, 4, 180–186.
7. Dehghani-Sanij, A.R.; Tharumalingam, E.; Dusseault, M.B.; Fraser, R. Study of energy storage systems and environmental challenges of batteries. *Renew. Sustain. Energy Rev.* 2019, 104, 192–208.
8. Yang, Z.; Zhang, J.; Kintner-Meyer, M.C.; Lu, X.; Choi, D.; Lemmon, J.P.; Liu, J. Electrochemical Energy Storage for Green Grid. *Chem. Rev.* 2011, 111, 3577–3613.
9. Ciez, R.E.; Whitacre, J.F. Examining different recycling processes for lithium-ion batteries. *Nat. Sustain.* 2019, 2, 148–156.
10. Ellingsen, L.A.-W.; Hung, C.R.; Strømman, A.H. Identifying key assumptions and differences in life cycle assessment studies of lithium-ion traction batteries with focus on greenhouse gas emissions. *Transp. Res. Part D Transp. Environ.* 2017, 55, 82–90.
11. Nishi, Y. Lithium ion secondary batteries; past 10 years and the future. *J. Power Sources* 2001, 100, 101–106.
12. Tariq, M.; Maswood, A.I.; Gajanayake, C.J.; Gupta, A.K. Aircraft batteries: Current trend towards more electric aircraft. *IET Electr. Syst. Transp.* 2017, 7, 93–103.
13. Lee, J.-W.; Anguchamy, Y.K.; Popov, B.N. Simulation of charge–discharge cycling of lithium-ion batteries under low-earth-orbit conditions. *J. Power Sources* 2006, 162, 1395–1400.
14. Ratnakumar, B.V.; Smart, M.C.; Kindler, A.; Frank, H.; Ewell, R.; Surampudi, S. Lithium batteries for aerospace applications: 2003 Mars Exploration Rover. *J. Power Sources* 2003, 119, 906–910.
15. Miao, Y.; Hynan, P.; Von Jouanne, A.; Yokochi, A. Current Li-Ion Battery Technologies in Electric Vehicles and Opportunities for Advancements. *Energies* 2019, 12, 1074.
16. Scrosati, B.; Garche, J. Lithium batteries: Status, prospects and future. *J. Power Sources* 2010, 195, 2419–2430.
17. Quartarone, E.; Mustarelli, P. Electrolytes for solid-state lithium rechargeable batteries: Recent advances and perspectives. *Chem. Soc. Rev.* 2011, 40, 2525–2540.
18. Chen, S.; Wen, K.; Fan, J.; Bando, Y.; Golberg, D. Progress and future prospects of high-voltage and high-safety electrolytes in advanced lithium batteries: From liquid to solid electrolytes. *J. Mater. Chem. A* 2018, 6, 11631–11663.

19. Zhang, H.; Zhao, H.; Khan, M.A.; Zou, W.; Xu, J.; Zhang, L.; Zhang, J. Recent progress in advanced electrode materials, separators and electrolytes for lithium batteries. *J. Mater. Chem. A* 2018, 6, 20564–20620.
20. Ozdemir, U.; Aktas, Y.O.; Vuruskan, A.; Dereli, Y.; Tarhan, A.F.; Demirbag, K.; Erdem, A.; Kalaycioglu, G.D.; Ozkol, I.; Inalhan, G. Design of a Commercial Hybrid VTOL UAV System. *J. Intell. Robot. Syst.* 2014, 74, 371–393.
21. Sun, Y.; Guan, P.; Liu, Y.; Xu, H.; Li, S.; Chu, D. Recent Progress in Lithium Lanthanum Titanate Electrolyte towards All Solid-State Lithium Ion Secondary Battery. *Crit. Rev. Solid State Mater. Sci.* 2019, 44, 265–282.
22. Sun, C.; Liu, J.; Gong, Y.; Wilkinson, D.P.; Zhang, J. Recent advances in all-solid-state rechargeable lithium batteries. *Nano Energy* 2017, 33, 363–386.
23. Mauger, A.; Julien, C.M.; Paolella, A.; Armand, M.; Zaghib, K. Building Better Batteries in the Solid State: A Review. *Materials* 2019, 12, 3892.
24. US Drive. Electrochemical Energy Storage Technical Team Roadmap (September 2017); US Drive: Washington, WA, USA, 2017.
25. Guan, X.; Wu, Q.; Zhang, X.; Guo, X.; Li, C.; Xu, J. In-situ crosslinked single ion gel polymer electrolyte with superior performances for lithium metal batteries. *Chem. Eng. J.* 2020, 382, 122935.
26. Lv, F.; Wang, Z.; Shi, L.; Zhu, J.; Edström, K.; Mindemark, J.; Yuan, S. Challenges and development of composite solid-state electrolytes for high-performance lithium ion batteries. *J. Power Sources* 2019, 441, 227175.
27. Tan, S.; Walus, S.; Hilborn, J.; Gustafsson, T.; Brandell, D. Poly(ether amine) and cross-linked poly(propylene oxide) diacrylate thin-film polymer electrolyte for 3D-microbatteries. *Electrochim. Commun.* 2010, 12, 1498–1500.
28. Scheers, J.; Fantini, S.; Johansson, P. A review of electrolytes for lithium–sulphur batteries. *J. Power Sources* 2014, 255, 204–218.
29. Mindemark, J.; Lacey, M.J.; Bowden, T.; Brandell, D. Beyond PEO—Alternative host materials for Li<sup>+</sup>-conducting solid polymer electrolytes. *Prog. Polym. Sci.* 2018, 81, 114–143.
30. Stepniak, I.; Andrzejewska, E.; Dembna, A.; Galinski, M. Characterization and application of N-methyl-N-propylpiperidinium bis(trifluoromethanesulfonyl)imide ionic liquid-based gel polymer electrolyte prepared in situ by photopolymerization method in lithium ion batteries. *Electrochim. Acta* 2014, 121, 27–33.
31. Röchow, E.T.; Coeler, M.; Pospiech, D.; Kobsch, O.; Mechtaeva, E.; Vogel, R.; Voit, B.; Nikolowski, K.; Wolter, M. In Situ Preparation of Crosslinked Polymer Electrolytes for Lithium Ion

- Batteries: A Comparison of Monomer Systems. *Polymers* 2020, 12, 1707.
32. Ma, C.; Cui, W.; Liu, X.; Ding, Y.; Wang, Y. In situ preparation of gel polymer electrolyte for lithium batteries: Progress and perspectives. *InfoMat* 2021, 1–16.
33. Zaghib, K.; Zhu, W.; Kaboli, S.; Demers, H.; Trudeau, M.; Paolella, A.; Guerfi, A.; Julien, C.M.; Mauger, A.; Armand, M.; et al. (Invited) In Operando and in Situ techniques for Intercalation Compounds in Li-Ion and All-Solid-State Batteries. In *ECS Meeting Abstracts*; No. 1; IOP Publishing: Bristol, UK, 2020; p. 16.
34. Mindemark, J.; Sun, B.; Törmä, E.; Brandell, D. High-performance solid polymer electrolytes for lithium batteries operational at ambient temperature. *J. Power Sources* 2015, 298, 166–170.
35. Wu, H.; Yu, G.; Pan, L.; Liu, N.; McDowell, M.T.; Bao, Z.; Cui, Y. Stable Li-ion battery anodes by in-situ polymerization of conducting hydrogel to conformally coat silicon nanoparticles. *Nat. Commun.* 2013, 4, 1–6.
36. Li, S.; Zhang, S.Q.; Shen, L.; Liu, Q.; Ma, J.B.; Lv, W.; He, Y.; Yang, Q.H. Progress and Perspective of Ceramic/Polymer Composite Solid Electrolytes for Lithium Batteries. *Adv. Sci.* 2020, 7, 1903088.
37. Yao, P.; Yu, H.; Ding, Z.; Liu, Y.; Lu, J.; Lavorgna, M.; Wu, J.; Liu, X. Review on Polymer-Based Composite Electrolytes for Lithium Batteries. *Front. Chem.* 2019, 7, 522.
38. Cao, C.; Li, Z.-B.; Wang, X.-L.; Zhao, X.-B.; Han, W.-Q. Recent Advances in Inorganic Solid Electrolytes for Lithium Batteries. *Front. Energy Res.* 2014, 2, 25.
39. Yu, X.; Manthiram, A. A review of composite polymer-ceramic electrolytes for lithium batteries. *Energy Storage Mater.* 2021, 34, 282–300.
40. Chen, L.; Li, Y.; Li, S.P.; Fan, L.Z.; Nan, C.W.; Goodenough, J.B. PEO/garnet composite electrolytes for solid-state lithium batteries: From “ceramic-in-polymer” to “polymer-in-ceramic”. *Nano Energy* 2018, 46, 176–184.
41. Falco, M.; Castro, L.; Nair, J.R.; Bella, F.; Bardé, F.; Meligrana, G.; Gerbaldi, C. UV-Cross-Linked Composite Polymer Electrolyte for High-Rate, Ambient Temperature Lithium Batteries. *ACS Appl. Energy Mater.* 2019, 2, 1600–1607.
42. Falco, M.; Simari, C.; Ferrara, C.; Nair, J.R.; Meligrana, G.; Bella, F.; Nicotera, I.; Mustarelli, P.; Winter, M.; Gerbaldi, C. Understanding the effect of UV-induced cross-linking on the physicochemical properties of highly performing PEO/LiTFSI-based polymer electrolytes. *Langmuir* 2019, 35, 8210–8219.
43. Shin, J.-H.; Henderson, W.A.; Passerini, S. PEO-Based Polymer Electrolytes with Ionic Liquids and Their Use in Lithium Metal-Polymer Electrolyte Batteries. *J. Electrochem. Soc.* 2005, 152, A978.

44. Kim, G.T.; Appeteccchi, G.B.; Carewska, M.; Joost, M.; Balducci, A.; Winter, M.; Passerini, S. UV cross-linked, lithium-conducting ternary polymer electrolytes containing ionic liquids. *J. Power Sources* 2010, 195, 6130–6137.
45. Bi, J.; Mu, D.; Wu, B.; Fu, J.; Yang, H.; Mu, G.; Zhang, L.; Wu, F. A hybrid solid electrolyte Li<sub>0.33</sub>La<sub>0.557</sub>TiO<sub>3</sub>/poly(acrylonitrile) membrane infiltrated with a succinonitrile-based electrolyte for solid state lithium-ion batteries. *J. Mater. Chem. A* 2020, 8, 706–713.
46. Al-Salih, H.; Huang, A.; Yim, C.-H.; Freytag, A.I.; Goward, G.R.; Baranova, E.; Abu-Lebdeh, Y. A Polymer-Rich Quaternary Composite Solid Electrolyte for Lithium Batteries. *J. Electrochem. Soc.* 2020, 167, 070557.
47. Yan, C.; Zhu, P.; Jia, H.; Zhu, J.; Selvan, R.K.; Li, Y.; Dong, X.; Du, Z.; Angunawela, I.; Wu, N.; et al. High-Performance 3-D Fiber Network Composite Electrolyte Enabled with Li-Ion Conducting Nanofibers and Amorphous PEO-Based Cross-Linked Polymer for Ambient All-Solid-State Lithium-Metal Batteries. *Adv. Fiber Mater.* 2019, 1, 46–60.
48. Li, B.; Su, Q.; Yu, L.; Wang, D.; Ding, S.; Zhang, M.; Du, G.; Xu, B. Li<sub>0.35</sub>La<sub>0.55</sub>TiO<sub>3</sub> Nanofibers Enhanced Poly(vinylidene fluoride)-Based Composite Polymer Electrolytes for All-Solid-State Batteries. *ACS Appl. Mater. Interfaces* 2019, 11, 42206–42213.
49. Liu, K.; Wu, M.; Wei, L.; Lin, Y.; Zhao, T. A composite solid electrolyte with a framework of vertically aligned perovskite for all-solid-state Li-metal batteries. *J. Membr. Sci.* 2020, 610, 118265.
50. Liu, K.; Zhang, R.; Sun, J.; Wu, M.; Zhao, T. Polyoxyethylene (PEO)|PEO–Perovskite|PEO Composite Electrolyte for All-Solid-State Lithium Metal Batteries. *ACS Appl. Mater. Interfaces* 2019, 11, 46930–46937.
51. Zhu, L.; Zhu, P.; Fang, Q.; Jing, M.; Shen, X.; Yang, L. A novel solid PEO/LLTO-nanowires polymer composite electrolyte for solid-state lithium-ion battery. *Electrochim. Acta* 2018, 292, 718–726.
52. Zhu, L.; Zhu, P.; Yao, S.; Shen, X.; Tu, F. High-performance solid PEO/PPC/LLTO-nanowires polymer composite electrolyte for solid-state lithium battery. *Int. J. Energy Res.* 2019, 43, 4854–4866.
53. He, K.-Q.; Zha, J.-W.; Du, P.; Cheng, S.H.-S.; Liu, C.; Dang, Z.-M.; Li, R.K.Y. Tailored high cycling performance in a solid polymer electrolyte with perovskite-type Li<sub>0.33</sub>La<sub>0.557</sub>TiO<sub>3</sub> nanofibers for all-solid-state lithium ion batteries. *Dalton Trans.* 2019, 48, 3263–3269.
54. Ding, C.; Fu, X.; Li, H.; Yang, J.; Lan, J.-L.; Yu, Y.; Zhong, W.-H.; Yang, X. An Ultrarobust Composite Gel Electrolyte Stabilizing Ion Deposition for Long-Life Lithium Metal Batteries. *Adv. Funct. Mater.* 2019, 29, 1904547.

55. Li, R.; Liao, K.; Zhou, W.; Li, X.; Meng, D.; Cai, R.; Shao, Z. Realizing fourfold enhancement in conductivity of perovskite  $\text{Li}_{0.33}\text{La}_{0.557}\text{TiO}_3$  electrolyte membrane via a Sr and Ta co-doping strategy. *J. Membr. Sci.* 2019, **582**, 194–202.
56. Meesala, Y.; Jena, A.; Chang, H.; Liu, R.-S. Recent Advancements in Li-Ion Conductors for All-Solid-State Li-Ion Batteries. *ACS Energy Lett.* 2017, **2**, 2734–2751.
57. Inaguma, Y.; Liquan, C.; Itoh, M.; Nakamura, T.; Uchida, T.; Ikuta, H.; Wakihara, M. High ionic conductivity in lithium lanthanum titanate. *Solid State Commun.* 1993, **86**, 689–693.
58. Chen, C.H.; Amine, K. Ionic conductivity, lithium insertion and extraction of lanthanum lithium titanate. *Solid State Ion.* 2001, **144**, 51–57.
59. Deng, D. Li-ion batteries: Basics, progress, and challenges. *Energy Sci. Eng.* 2015, **3**, 385–418.
60. Kokal, I. Solid State Electrolytes for All Solid State 3D Lithium Ion Batteries. Ph.D. Thesis, Eindhoven University of Technology, Eindhoven, The Netherlands, 6 November 2012.
61. Inaguma, Y.; Itoh, M. Influences of carrier concentration and site percolation on lithium ion conductivity in perovskite-type oxides. *Solid State Ion.* 1996, **86**, 257–260.
62. Kim, S.; Hirayama, M.; Cho, W.; Kim, K.; Kobayashi, T.; Kaneko, R.; Suzuki, K.; Kanno, R. Low temperature synthesis and ionic conductivity of the epitaxial  $\text{Li}_{0.17}\text{La}_{0.61}\text{TiO}_3$  film electrolyte. *CrystEngComm* 2014, **16**, 1044–1049.
63. Abhilash, K.; Sivaraj, P.; Selvin, P.; Nalini, B.; Somasundaram, K. Investigation on spin coated LLTO thin film nano-electrolytes for rechargeable lithium ion batteries. *Ceram. Int.* 2015, **41**, 13823–13829.
64. Geng, H.X.; Mei, A.; Dong, C.; Lin, Y.H.; Nan, C.W. Investigation of structure and electrical properties of  $\text{Li}_{0.5}\text{La}_{0.5}\text{TiO}_3$  ceramics via microwave sintering. *J. Alloy. Compd.* 2009, **481**, 555–558.
65. Ling, M.; Jiang, Y.; Huang, Y.; Zhou, Y.; Zhu, X. Enhancement of ionic conductivity in  $\text{Li}_{0.5}\text{La}_{0.5}\text{TiO}_3$  with Ag nanoparticles. *J. Mater. Sci.* 2020, **55**, 3750–3759.
66. Mei, A.; Wang, X.-L.; Lan, J.; Feng, Y.-C.; Geng, H.-X.; Lin, Y.-H.; Nan, C.-W. Role of amorphous boundary layer in enhancing ionic conductivity of lithium–lanthanum–titanate electrolyte. *Electrochim. Acta* 2010, **55**, 2958–2963.
67. Zhang, S.; Zhao, H.; Guo, J.; Du, Z.; Wang, J.; Świerczek, K. Characterization of Sr-doped lithium lanthanum titanate with improved transport properties. *Solid State Ion.* 2019, **336**, 39–46.
68. Lee, S.-J.; Bae, J.-J.; Son, J.-T. Structural and Electrical Effects of Y-doped  $\text{Li}_{0.33}\text{La}_{0.56-x}\text{Y}_x\text{TiO}_3$  Solid Electrolytes on All-Solid-State Lithium Ion Batteries. *J. Korean Phys. Soc.* 2019, **74**, 73–77.

69. Jiang, Y.; Huang, Y.; Hu, Z.; Zhou, Y.; Zhu, J.; Zhu, X. Effects of B-site ion ( $\text{Nb}^{5+}$ ) substitution on the microstructure and ionic conductivity of  $\text{Li}_{0.5}\text{La}_{0.5}\text{TiO}_3$  solid electrolytes. *Ferroelectrics* 2020, 554, 89–96.

Retrieved from <https://encyclopedia.pub/entry/history/show/38623>